

# On the possibility of detecting Solar $pp$ -neutrino with a large volume liquid organic scintillator detector.\*

1st November 2018

A.V.Derbin<sup>1</sup>, O.Yu.Smirnov<sup>2,3</sup>, and O.A.Zaimidoroga<sup>3</sup>

## Abstract

It is shown that a large volume liquid organic scintillator detector with an energy resolution of 10 keV at 200 keV ( $1\sigma$ ) will be sensitive to solar  $pp$ -neutrino, if operated at the target radiopurity levels for the Borexino detector, or the solar neutrino project of KamLAND.

## 1 Introduction

Present information on the solar neutrino spectrum is based on the very tail of the total neutrino flux (about 0.2%). The low energy part of the spectrum, and in particular  $pp$ -neutrino flux, has not been measured directly yet. After the observation of reactor neutrino oscillations by the KamLAND collaboration [1], the spectrometry of the low energy solar neutrinos is important for the confirmation of the LMA MSW scenario, for the restricting of the allowed LMA parameters region [2], as well as for the search of the neutrino nonstandard properties.

The  $pp$  neutrinos measurement is a critical test of stellar evolution theory and of neutrino oscillation solutions. The  $pp$ -neutrino flux is predicted by the Standard Solar Model (SSM) with a precision of the order of 1%, in contrast to the 20% precision predictions of the high energy neutrino flux from the  $^8B$ . A discussion of the physics potential of the  $pp$  solar neutrino flux can be found in [3],[4] and [5]. A number of projects aiming to build  $pp$ -neutrino spectrometers are in the different stages of research and development.

---

\*Contributed paper to the Nonaccelerating New Neutrino Physics conference, NANP-2003, Dubna. To appear in Phys.At.Nucl.(2004)

<sup>1</sup>St. Petersburg Nuclear Physics Institute - Gatchina, Russia.

<sup>2</sup>Corresponding author: E-mail: osmirnov@jinr.ru;smirnov@lngs.infn.it

<sup>3</sup>Joint Institute for Nuclear Research, 141980 Dubna, Russia.

Table 1: Key characteristics of the solar neutrino projects sensitive to the  $pp$ -neutrino

Project (Reference)	Method	Threshold, keV	Resolution	Mass, t	Reaction	SSM pp events, $d^{-1}$
LENS (Yb) [6]	$^{176}\text{Yb}$ , LS	301 ( $\nu$ )	7% @ 1 MeV	20 (8% in nat Yb)	$^{176}\text{Yb} + \nu_e \rightarrow$ $^{176}\text{Lu} + e^-$	0.5
LENS (In) [7]	$^{115}\text{In}$ LS	118( $\nu$ )	18% @100 keV	20	$^{115}\text{In} + \nu_e \rightarrow$ $^{115}\text{Sn}^*(613) + e^-$	1.4 $\epsilon(pp) = 0.25$
GENIUS [8]	$^{76}\text{Ge}$ Scatt	11( $e^-$ ) 59( $\nu$ )	0.3% @ 300 keV	1 10	$\nu + e^- \rightarrow$ $\nu + e^-$	1.8 18
HERON [9]	Superfluid $^4\text{He}$ Rotons/phonons+UV	50( $e^-$ ) 141( $\nu$ )	10% @50 keV	20 (28)	$\nu + e^- \rightarrow$ $\nu + e^-$	5.5 (LMA)
XMASS [10]	Liquid Xe Scintill	50( $e^-$ ) 141( $\nu$ )	11% @ 300 keV	10	$\nu + e^- \rightarrow$ $\nu + e^-$	10
HELLAZ [11]	He (5 atm), TPC	100( $e^-$ ) 217( $\nu$ )	6% @800 keV	2000 $m^3$	$\nu + e^- \rightarrow$ $\nu + e^-$	7
MOON [12]	Drift Chambers	168( $\nu$ )	12.4% FWHH @ 1 MeV	3.3	$\nu_e + ^{100}\text{Mo} \rightarrow$ $^{100}\text{Tc} + e^-$	1.1
MUNU [13]	TPC, $\text{CF}_4$ Direction	100( $e^-$ ) 217( $\nu$ )	16% FWHH @ 1 MeV	0.74 (200 $m^3$ )	$\nu + e^- \rightarrow$ $\nu + e^-$	0.5
NEON [14]	He,Ne Scintill	20( $e^-$ ) 82( $\nu$ )	16% FWHH @ 100 keV	10	$\nu + e^- \rightarrow$ $\nu + e^-$	18
Present work	LS	170( $e^-$ ) 310( $\nu$ )	10.5 keV @ 200 keV	10	$\nu + e^- \rightarrow$ $\nu + e^-$	1.8 1.1 (LMA)

The principal characteristics of the existing proposals [6]-[14] are shown in Table 1. The operating gallium radiochemical experiments sensitive to solar  $pp$ - neutrinos (SAGE [15] and GALLEX [16]) are not cited in the table, because they do not provide spectrographic information.

Table 2: Achived and targeted purities in the Borexino and KamLAND solar neutrino projects.

	CTF of Borexino [39, 20, 21]	Borexino goals, [19]	KamLAND [30]	KamLAND goals, [30]
$^{14}C$	$2 \times 10^{-18}$ g/g	$\sim 10^{-18}$ g/g	No data	
$^{238}U$	$< 4.8 \times 10^{-16}$ g/g	$\sim 10^{-16}$ g/g ( $1 \mu\text{Bq}/\text{m}^3$ )	$3.5 \times 10^{-18}$ g/g	$\sim 10^{-16}$ g/g
$^{232}Th$	$< 8.4 \times 10^{-16}$ g/g	$\sim 10^{-16}$ g/g	$5.2 \times 10^{-17}$ g/g	$\sim 10^{-16}$ g/g
$^{40}K$	$\leq 10^{-15}$ g/g	$\sim 10^{-18}$ g/g	$2.7 \times 10^{-16}$ g/g	$\leq 10^{-18}$ g/g
$^{210}Pb$	$< 500 \mu\text{Bq}/\text{t}$	$\sim 1 \mu\text{Bq}/\text{m}^3$	$\simeq 10^{-20}$ g/g	$5 \times 10^{-25}$ g/g ( $1 \mu\text{Bq}/\text{m}^3$ )
$^{85}Kr$	$< 600 \mu\text{Bq}/\text{t}$	$\sim 1 \mu\text{Bq}/\text{m}^3$	$0.7 \text{ Bq}/\text{m}^3$	$1 \mu\text{Bq}/\text{m}^3$
$^{39}Ar$	$< 800 \mu\text{Bq}/\text{t}$	$\sim 1 \mu\text{Bq}/\text{m}^3$		
$^{222}Rn$	$(3.5 \pm 1.4) \times 10^{-16}$ g/g ( $\sim 3 \mu\text{Bq}/\text{m}^3$ )	$\sim 10^{-16}$ g/g	$0.03 \mu\text{Bq}/\text{m}^3$	$1 \mu\text{Bq}/\text{m}^3$

The main problem in the neutrino detection is the very small cross sections of the neutrino interactions with matter, this demands a large detectors with a very low intrinsic background. Below we summarize briefly the achievements in the purification of the liquid organic scintillators, and on the basis of the developed techniques propose a high resolution detector, filled with a liquid organic scintillator, with an energy threshold as low as 170-180 keV, capable of registering solar  $pp$ -neutrinos. A preliminary description has been reported in [17].

## 2 Purities achieved with liquid scintillator detectors

For the present moment the record on liquid organic scintillator purity with a large scale sample has been achieved with the Borexino [18, 19] Counting Test Facility (CTF) and KamLAND detector [1]. The available data are summarized in table 2. While the CTF is a prototype detector operating with 4 tones of liquid scintillator [20, 21], the KamLAND detector is loaded with 1000 tones of the liquid scintillator. Both detectors demonstrate very good purification of the scintillator for  $U - Th$  and  $^{222}Rn$ . The values cited in table 2 for the  $^{238}U$  and  $^{232}Th$  content are obtained by counting the number of the decay sequences from  $^{214}Bi$  and  $^{212}Bi$  in the assumption of secular equilibrium. A precise measurement of the abundance of  $^{40}K$  was not possible with CTF because of the sensitivity level, but is

expected to be much better because of the high efficiency of water extraction for the removal of  $K$  ions [19]. The investigation performed in the frame of the Borexino programme shows that the content of the  $^{85}Kr$  and  $^{39}Ar$  can be significantly decreased by the proper choice of the  $N_2$  for the stripping. The goals for the purity in both Borexino and KamLAND project for the observation of the solar neutrinos are similar.

The importance of the purification of the liquid scintillator from the  $^{39}Ar$  and  $^{85}Kr$  was understood during the operation of the CTF.

### 3 The design of the detector

Even in the case that the desired purity can be achieved in the future Borexino and KamLAND experiments, the direct measurements in the  $pp$ -neutrino energy region are impossible with these big detectors. In fact, the presence of the beta-decaying  $^{14}C$  isotope in the liquid organic scintillator sets a lower threshold on the detector sensitivity. The measured content of the  $^{14}C$  in the liquid scintillator used in the CTF detector was at the level of  $2 \times 10^{-18}$  g/g with respect to the  $^{12}C$  content [23], and this is the only measurement available at such a low concentration. Though the end point of the  $^{14}C$   $\beta$ - decay is only 156 keV, the energy resolutions of the CTF, as well as Borexino and KamLAND, are not good enough at this energy in order to set a threshold lower than 250 keV.

Thus, the efforts should be concentrated on the construction of a compact detector with the highest possible energy and spatial resolution. We suggest to use PMTs supplied with hexagonal light concentrators in order to provide  $4\pi$  coverage, in comparison to 21% for CTF and 30% for Borexino and KamLAND. Additional energy resolution improvement (about 15%) in the low energy region can be achieved by using an energy reconstruction technique discussed in [24]. Good spatial resolution is needed in order to provide an active shielding from the external background, mainly gammas with energy 1.45 MeV coming from the  $^{40}K$  decay in the PMT material. The additional passive shielding with 200 cm of ultrapure water is considered in the present design.

The possible geometry of the detector is presented in the Fig.1 in comparison with Borexino and CTF sketches. The inner vessel is a transparent spherical nylon bag with a radius of 240 cm, containing 60 tons of ultrapure pseudocumene with 1.5 g/g of PPO. The active shielding is provided by 100 cm of the outer layer of scintillator. The 800 PMTs are mounted on an open structure at a distance of 440 cm from the detector's center (distance is counted from the PMT photocathode). We considered also the use of the 8" ETL9351 series photomultiplier [25]. The comparison of the geometrical parameters of Borexino, CTF and the proposed detector is presented in the Table 3.

The choice of the geometry is motivated by the following reasons:

- the highest possible energy and spatial resolution;
- the detector should fit in the existing CTF external tank, which is 10 m height and 11 m in diameter;

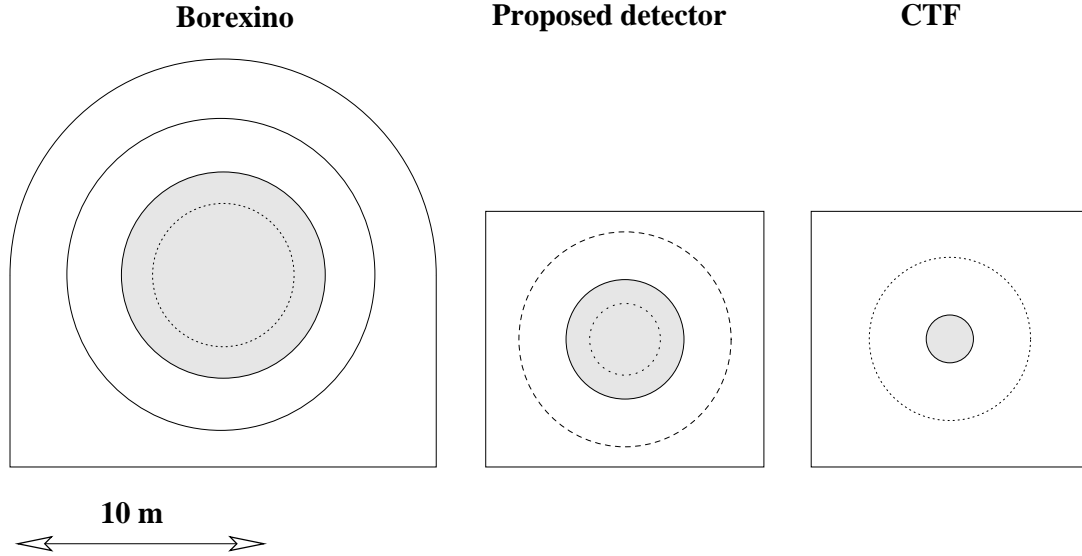


Figure 1: Comparison of the geometry of the Borexino, CTF and proposed detectors. The inner vessel with scintillator is shown with a gray colour. The dashed line inside the inner vessel defines the fiducial volume, the outer layer protects the fiducial volume from the external gammas. PMTs are uniformly distributed over the surface shown with a solid line on the Borexino drawing and with a dashed line on the two others.

- the light registration system should provide maximum possible geometrical coverage with a minimal number of PMTs required;
- the active shielding of the fiducial volume is provided by at least 100 cm of scintillator;
- the passive shielding against the gammas originating from the PMT impurities is provided by 200 cm of ultrapure water;
- the fiducial volume of the detector should be of the order of 10 tons;
- the inner vessel size should be as small as possible in order to avoid the loss of light in the scintillator and to provide better detector uniformity;
- to lower the detector's threshold ( $< 35$  keV) in order to acquire the  $^{14}\text{C}$  spectrum shape without deformations caused by the threshold effects.

Table 3: Comparison of the main features of the CTF, Borexino and the proposed detector. Some data for the KamLand detector are shown for comparison. Because of the higher threshold (400 keV), the energy and spatial resolutions are not estimated for KamLand.

Parameter	CTF	Borexino	KamLand (Solar $\nu$ project)	Proposed detector
Geometrical coverage	21%	30%	34%	$\cong 100\%$
Light yield (p.e./MeV)	360	400	320	1800
Light yield per PMT for the event at the detector's center $\mu_0$ , p.e./MeV	3.6	0.25	$\geq 0.25$	2.25
Energy resolution @ 200 keV, keV $(\sim \frac{1}{\sqrt{\text{Lightyield}}})$	27	26		10.5
Threshold, keV	250	250	400	170
Muon veto PMTs	16	200		50
PMTs number	100	2200	1325 (17'') + 554 (20'')	800
Total natural K content in the PMTs, g	8	176		64
Distance between the PMTs and detector's center, cm	330	675	825	440
Spatial resolution @ 200 keV, cm $(\sim \langle \frac{1}{\sqrt{N_{hit}}} \rangle \cong \frac{1}{\sqrt{N_{PM}(1-e^{-0.2\mu_0})}})$	20	45		8

A larger size detector is an unfavourable solution because of the huge number of the PMTs necessary to provide  $4\pi$  coverage. The big inner vessel volume in turn decreases the amount of the light escaping from the interior part of the detector. The spatial reconstruction of the lower energy events is complicated because of multiple absorption and reemission of the light on the way to the PMTs with a characteristic length of 1 m [26].

The detector should be supplied with an external muon veto system. The muon veto system consisting of about 50 additional PMTs can be mounted on the top and on the bottom of the cylindrical external tank. The muon recognition efficiency should be at the level of 99.99% in order to guarantee missed muons count  $< 0.1$  per day. The muons flux at the LNGS underground laboratory is about 7 times less than at the Kamioka site.

## 4 Detector energy resolution

A detailed analysis of the large volume liquid scintillator detector energy resolution can be found in [24] and [27]. We give here a brief overview of the main results because of the

importance for further discussion. Taking into account the dependence of the registered charge on energy one can write for the CTF charge resolution<sup>1</sup>:

$$\frac{\sigma_Q}{Q} = \sqrt{\frac{1 + \overline{v_1}}{A \cdot E \cdot f(k_B, E) \cdot v_f}} + v(p), \quad (1)$$

where

$\overline{v_1} = \frac{1}{N_{PM}} \sum_{i=1}^{N_{PM}} s_i v_{1_i}$  is the relative variance of the PMT single photoelectron charge spectrum ( $v_{1_i}$ ) averaged over all CTF PMTs ( $N_{PM}$ ), taking into account the relative sensitivity  $s_i$  of the  $i$ -th PMT;

$v(p)$  is the parameter which takes into account the variance of the signal for the source uniformly distributed over the detector's volume. Because of the detector's spherical symmetry one can describe the dependence of the registered charge on the distance from the event to the detector's center  $\mathbf{r}$  with a function  $Q(r)$  of a single parameter  $\mathbf{r}$ ,  $Q(r) = Q_0 f_R(r)$ , where  $Q_0$  is the charge collected for an event of the same energy occurring at the detector's center. The  $v(p)$  parameter is the relative variance of the factor  $f_R(r)$  describing the radial dependence of the registered charge:

$$v(p) \equiv \frac{\langle f_R^2(r) \rangle_V}{\langle f_R(r) \rangle_V^2} - 1; \quad (2)$$

$v_f$  is volume factor, coming from the averaging of the signals over the CTF volume,  $v_f \equiv \frac{\langle Q(r) \rangle_V}{Q_0}$ .

$f(k_B, E)$  is a function taking into account the suppression of the light yield at low energies, the so called ionization quenching.

The coefficient  $A$  linking the event energy and the total collected charge is called the light (or photoelectron) yield. The light yield for electrons can be considered linear with respect to its energy only for energies above 1 MeV. At low energies the phenomenon of "ionization quenching" violates the linear dependence of the light yield versus energy [28]. The deviations from the linear law can be taken into account by the ionization deficit function  $f(k_B, E)$ , where  $k_B$  is Birks' constant. For the calculations of the ionization quenching effect for PC scintillator we used the KB program from the CPC library [29].

For the details of the meaning of the parameters see [24] and [27]. For the signal calculation we used the following parameters:  $A = 1800$  p.e./MeV,  $v_1 = 0$ ,  $v_f = 1$ ,  $v(p) = 2.3 \times 10^{-3}$ ,  $k_B = 0.0167$ .

The signal  $S(Q)$  registered by the detector is the convolution of the "pure" signal spectrum  $S_0(Q)$  with the detector's resolution:

$$S(Q) = N_0 \int S_0(E(Q')) \frac{dE}{dQ} Res(Q, Q') dQ' \quad (3)$$

---

<sup>1</sup>This is the case when no energy reconstruction is performed and the energy is defined by dividing the total registered charge by the p.e. yield  $A$ :  $E = \frac{Q}{A}$ .

where  $Res(Q, Q') = \frac{1}{\sqrt{2\pi}\sigma_Q} e^{-\frac{1}{2}(\frac{Q-Q'}{\sigma_Q})^2}$  is the detector response function, and  $\sigma_Q$  is defined by (1).

## 5 Backgrounds

The sensitivity of the detector to the solar  $pp$ -neutrino depends on the background level in the 170– 250- keV energy window. As in Borexino, CTF ([18], [20]) and the KamLAND solar neutrino project [30], the main sources of background are

- internal background, including  $^{14}\text{C}$  beta- decay counts in the neutrino window;
- background from the radon dissolved in the buffer ;
- external gamma background;
- cosmic ray background.

We considered the contamination of the liquid scintillator with the radionuclides on the levels given in table 2 for Borexino.

In the following subsections we give an estimate of the background contribution from each source, showing that the main contribution into the background is due to the internal radionuclide decays. The Monte- Carlo method has been used in our calculations in order to simulate the detector response to the background events. The code is split in two parts: the electron-gamma shower simulation (EG code) and the simulation of the registered charge and position (REG code). The EG code generates a random position event with a random initial direction (for gammas) and follows the gamma- electron shower using the EGS-4 code[31]. The electrons and alphas are not propagated in the program and are considered to be point-like, with the position at the initial coordinates. The mean registered charge corresponding to the electron's energy  $E_e$  is calculated by

$$Q_e = A \cdot E_e \cdot f(k_B, E) \cdot f_R(r), \quad (4)$$

where  $f_R(r)$  is a factor, taking into account the dependence of the registered charge on the distance from the detector's center, and  $f(k_B, E_e)$  is the quenching factor for electrons.

The factor  $f_R(r)$  was estimated with the Monte Carlo method, simulating the light collection from the source, placed at different distances from the detector's center. The quenching factor  $k_B = 0.0167$  was independently measured for the scintillator on the base of pseudocumene (PC) [32]. The value is in agreement with a high statistics fit of the  $^{14}\text{C}$   $\beta$ -spectrum of the CTF data.

The mean registered charge corresponding to an alpha of energy  $E$  is calculated by

$$Q_\alpha = A \cdot E_\alpha \cdot f_\alpha(E) \cdot f_R(r), \quad (5)$$



where  $f_\alpha(E)$  is the quenching factor for alphas. The following approximation of the quenching factor  $f_\alpha(E)$  was used for the simulations with PC [33]:

$$f_\alpha(E) = \frac{1}{20.3 - 1.3 \cdot E},$$

where alpha energy  $E$  is measured in MeV.

The gammas were propagated using the EGS-4 code. As soon as an electron of energy  $E_e$  appears inside the scintillator, the corresponding charge is calculated:

$$\Delta Q_i = A \cdot E_{e_i} \cdot f(k_B, E_e) \cdot f_R(r_i). \quad (6)$$

The total mean collected charge is defined when the gamma is discarded by the EG code, summing individual deposits:

$$Q_\gamma = \sum \Delta Q_i.$$

The weighted position is assigned to the final gamma:

$$x_w = \frac{\sum \Delta Q_i \cdot x_i}{\sum \Delta Q_i}, \quad (7)$$

where  $\Delta Q_i$  and  $x_i$  are the charge deposited for the  $i$ -th electron at the position  $\{x_i, y_i, z_i\}$ . The same rule is applied for the  $y_w$  and  $z_w$  coordinates.

In the next step a random charge is generated according to the normal distribution with a mean value of  $Q = \sum \Delta Q$  and with variance  $\sigma_Q = \sqrt{(1 + \bar{v}_1) \cdot Q}$ . Finally, the radial reconstruction is simulated taking into account the energy dependence of the reconstruction precision. It is assumed that the reconstruction precision is defined by the number of PMTs fired in an event, and that the reconstruction precision doesn't depend on the position. These two facts were confirmed by the measurements with an artificial radon source inserted in the CTF-I and CTF-II detectors [21]. The reconstruction precision for the radon events can be obtained either by the direct measurement with a source or by fitting the distribution of the radon events. The mean number of channels fired for an event with an energy  $E$  at the detector's center is:

$$\langle N \rangle = N_{PMT}(1 - e^{-\mu_0}), \quad (8)$$

where  $\mu_0$  is the mean number of photoelectrons registered by one PMT in the event and  $N_{PMT}$  is the total number of the PMTs. If we assume that the reconstruction precision is defined by the mean number of fired channels, then the reconstruction precision is:

$$\sigma_R(E) = \sigma_R(E_{ref}) \cdot \sqrt{\frac{\langle N(E_{ref}) \rangle}{\langle N(E) \rangle}}, \quad (9)$$

where  $\sigma_R(E_{ref})$  is the spatial resolution for a monoenergetic source with energy  $E_{ref}$ . We used as reference the values obtained with the CTF-I detector with a  $^{214}Po$  source:  $\sigma_R(0.751 \text{ keV}) = 12.3 \pm 0.04 \text{ cm}$  [21].

We expect less than 1 event per day due to the internal background in 10 tons of scintillator in the energy window 170-250 keV. The better energy and spatial resolutions of the detector will permit us to improve the  $\alpha/\beta$  discrimination capability in comparison to CTF. The very low energy threshold together with better energy and spatial resolutions will allow as well to improve the selection of the sequential decays from the radioactive chains.

## 5.1 Internal background from the metallic ions and radioactive noble gases

The contamination of the scintillator with natural radioactive isotopes gives a total rate of 1320 events/year in the energy window 170-750 keV with the following assumptions:

- the content of radioactive isotopes in the scintillator is given by table 2;
- secular equilibrium of the radioactive elements in the decay chains;
- a 95% capability to reject alphas ( $\alpha/\beta$ - discrimination technique based on the different shape of the detector response to  $\alpha$  and  $\beta$ );
- 95% rejection efficiency of the delayed coincidence method based on the tagging of the  $^{214}\text{Bi} - ^{214}\text{Po}$  decay chain;
- 95% efficiency of the statistical subtraction method based on the deducing the isotopes in the  $Rn$  chain preceding the Bi-Po coincidence.

A more complete discussion of the background reduction techniques can be found in [18]. The excellent detector's resolution can improve the efficiency of all the techniques.

Only 230 events of the total amount falls into the 170– 250- keV energy window.

## 5.2 Internal background from $^{14}\text{C}$ decays

### 5.2.1 $^{14}\text{C}$ spectrum

The major part of the background in liquid organic scintillators in the energy region up to 200 keV is the  $\beta$ -activity of  $^{14}\text{C}$ . The  $\beta$ -decay of  $^{14}\text{C}$  is an allowed ground-state to ground-state ( $0^+ \rightarrow 1^+$ ) Gamow– Teller transition with an endpoint energy of  $E_0 = 156$  keV and half life of 5730 yr. For the evaluation of the  $^{14}\text{C}$  background we used the  $\beta$ - energy spectrum with a massless neutrino in the form [34]:

$$dN(E) \sim F(Z, E)C(E)pE(Q - E)^2dE \quad (10)$$

where

$E$  and  $P$  are the total electron energy and momentum;

$F(E, Z)$  is the Fermi function with correction of screening by atomic electrons;

$C(E)$  contains departures from allowed shape.

For  $F(E, Z)$  we used the function from [35] which agrees with tabulated values of the relativistic calculation [36]. A screening correction has been made using Rose's method [37] with screening potential  $V_0 = 495$  eV. The  $^{14}\text{C}$  spectrum shape factor can be parametrized as  $C(E) = 1 + \alpha E$ . In our calculation we used the value  $\alpha = -0.72$  [23].

The total amount of the events in the 172– 250- keV energy window, with the energy resolution corresponding to 1800 p.e./MeV, is 1500 ev/y/10 t if the  $^{14}\text{C}$  content is  $2 \times 10^{-18}$  g/g. This is the content measured at the CTF-I setup [23].

### 5.2.2 $^{14}\text{C}$ spectrum and the detector's threshold

In order to separate events from the background near the  $^{14}\text{C}$  spectrum end point, it is necessary to acquire the part of the spectrum under the physical threshold of the detector (170 keV). We propose to use the following technique for the detector triggering. First, the lower level trigger is produced as a coincidence of the signals from 20 PMTs in a 50 ns gate. This will give a negligible random coincidence rate at the level  $< 10^{-10}$  ev/y if all the PMTs have a dark rate less than 5 kHz. The high level trigger is produced if the total collected charge is greater than the preset threshold  $Q_{th}$ . The choice of this threshold will be defined by the resolution of the detector. Let us estimate the last quantity. The mean number of channels fired for an event with an energy  $E$  at the detector's center can be calculated using (8) with  $N_{PM} = 800$ . The solution of (8) for  $\langle N \rangle = 20$  will yield  $\mu_0 \simeq 0.025$ , i.e. a total collected charge of 20 p.e. This value is the detector threshold in the sense that only 50% of the events with an energy corresponding to this charge are registered. Of course, this causes a significant spectrum deformation near the threshold. In order to avoid these deformations one should set the threshold at a level that will cut the events with energies that are not providing 100% registration, i.e.  $Q_{th} + 3\sigma_{Q_{th}} = 20 + 3\sqrt{20} = 33.4$  p.e. This charge corresponds to approximately 35 keV if the ionization quenching at this energy is 50%. Though this calculation was performed for an event at the detector's center, and the real situation is complicated by the electronics threshold, it gives a value very close to the one obtained with the Monte Carlo simulation.

It is commonly assumed that the  $^{14}\text{C}$  content sets the limit on the sensitivity at the low energy region in liquid organic scintillators. A ratio as low as  $2 \times 10^{-18}$  g/g was achieved with CTF detector. There are indications that the content of  $^{14}\text{C}$  can be even smaller, of the order of  $10^{-21}$  g/g [38]<sup>2</sup>. In this case the  $^{14}\text{C}$  contribution in the background can be reduced by a factor 2000. It is interesting to study the dependence on the content of the  $^{14}\text{C}$  in the scintillator for the sensitivity of the detector to the pp- neutrinos. The results of the study are summarized in Table 4. One can see that the detector sensitivity varies rather slowly with the decrease of the  $^{14}\text{C}$  content in the scintillator. There are several reasons for this behaviour. First of all, the pp- neutrino rate is quite low and with minimal background contribution the statistical fluctuations of the pp- rate are the major source

---

<sup>2</sup>New petro-geological models allow such a low value; contamination with modern  $^{14}\text{C}$  in this case have to be excluded during petroleum refinement [38]. The existing CTF setup is a suitable device for the search of the organic LS with minimal  $^{14}\text{C}$  contamination.

Table 4: The effect of the  $^{14}\text{C}$  in the scintillator on the sensitivity of the detector to the SSM  $pp$ - neutrinos (in LMA MSW scenario). The data corresponds to a detectors mass of 10 tones and for 1 year of the data taking.

$^{14}\text{C}$ , g/g	$2 \times 10^{-18}$	$10^{-19}$	$10^{-20}$	$10^{-21}$
Threshold ( $\sqrt{bkg}=\text{eff}$ )	172 (40)	152	108	0
Threshold ( $2\sqrt{bkg}=\text{eff}$ )	178	163	140	0
Energy interval	172–250	150–250	150–250	150–250
$^{14}\text{C}$ events	1500	5383	538	54
Internal Background	228	287	287	287
pp (LMA)	412	705	705	705
Total $\nu$ 's (LMA)	668	1035	1035	1035

of the uncertainty. Another source of uncertainty is the irreducible internal background which becomes comparable to the  $^{14}\text{C}$  events contribution with the lower  $^{14}\text{C}$  content. The last reason is the lower threshold of the detector of about 25 keV, which can't be decreased without increasing the random electronics noise. In order to avoid the influence of the threshold effect on the spectrum shape it is necessary to set the software threshold even higher, to about 40 keV. Another motivation to set a higher software threshold is the presence of low energy external gammas which can be reconstructed inside the fiducial volume due to the poor spatial resolution at low energies.

We can conclude that lower  $^{14}\text{C}$  content would be desirable but is not critical for the detector sensitivity to  $pp$ - neutrinos.

### 5.2.3 $^{14}\text{C}$ pile-up events

A potential danger are the  $^{14}\text{C}$  pile-up events, i.e. events occurring sequentially within a coincidence window. Such events can in principle influence the  $^{14}\text{C}$  spectrum tail. The fraction of the  $^{14}\text{C}$  pile-up events with energies above 170 keV is about 5%. The total amount of pile-up events depends on the  $^{14}\text{C}$  relative abundance and on the coincidence window:

$$N_{p.u.} = \tau_{Gate} \times f_{14C}^2 \times T, \quad (11)$$

where  $T$  is the total time of the data taking,  $\tau_{Gate} = 60\text{ns}$  is the coincidence gate width, and  $f_{14C}$  is the frequency of the  $^{14}\text{C}$  events. For a  $^{14}\text{C}$  abundance of  $2 \times 10^{-18}$  g/g, the mean rate of the events caused by  $^{14}\text{C}$   $\beta$ - decay is 2.2Hz. With these values the number of pile-up events is 2.5 per day, and the number of events with energy greater then 170 keV is only about 0.13 per day.

The selection of point-like events provides a further possibility to suppress the amount

of these events by a factor of at least  $\left(\frac{\frac{4}{3}\pi(3\sigma_R)^3}{V_{FV}}\right)^2 = \left(\frac{3\sigma_R}{R_{FV}}\right)^6 \simeq 10^{-5}$ , where  $\sigma_R$  is the spatial resolution at 170 keV and  $R_{FV} = 140$  cm is the radius of the fiducial volume. Thus, one can conclude that pile-up events will not influence the shape of the  $^{14}\text{C}$  spectrum within the considered energy interval.

### 5.3 External gamma background

The external background counts are caused mainly by the radioactive contamination of the PMT glass with  $^{40}\text{K}$  and elements of the U-Th chain. The assumed content of the  $^{238}\text{U}$ ,  $^{232}\text{Th}$  and  $K_{nat}$  in the PMTs is 112  $\mu\text{g}/\text{PMT}$ , 47  $\mu\text{g}/\text{PMT}$  and 62  $\text{mg}/\text{PMT}$  respectively, which corresponds to the measured radioactive contamination of the phototubes produced with high purity glass [39]. We add 30% to these values to account for the radioactive contamination of the concentrator and PMT divider, sealing and support structure. Another source of external gammas is radon dissolved in the water buffer.

The results of a simulation show that a  $R < 150$  cm spatial cut will eliminate all the events in the neutrino window (170–250- keV). Nevertheless, in order to reduce the background from the penetrating gamma's we suggest to reduce the amount of the construction materials contributing to the background. A significant amount of the material in Borexino is contained in the mu-metal shield of the PMTs, which provides the screening of the PMTs against the terrestrial magnetic field. An alternative solution based on the PMTs orientation has been studied in [40]. The effect of the PMTs orientation is comparable to the one achieved with the PMT screening with the high magnetic permeability metal. Use of this technique could eliminate about 1 kg of material for each PMT in proximity to the inner vessel.

Another possibility to reduce the gamma background assumes the use of a different topology of the events produced by the electrons and gammas. The excellent spatial resolution of the detector will permit distinguishing point-like energy deposits for electrons from the distributed gamma events ( $\beta/\gamma$  discrimination). The study of the possibility of such discrimination for the Borexino detector is now in progress.

### 5.4 Cosmic ray induced background

The cosmic ray induced background can be subdivided into the three categories:

1. Muons crossing the water buffer of the detector, producing Cerenkov light;
2. Neutrons produced by muon interactions, and sequentially stopped in the water or the scintillator and emitting a 2.2 MeV annihilation gamma;
3. Secondary radioactive nuclei produced in the muon interactions inside the detector.

Most of the background counts associated with muons can be effectively removed by the muon identifying system (muon veto). One can use the time and spatial structure of the

muon induced events in order to recognize them. The muon identification procedure was able to recognize 95% of the muon induced events in the CTF-I detector [20]. We assume also the use of a set of PMTs situated on the top and bottom of the cylindrical external tank that will increase the muon identification to a value approaching 100%.

Some of the radioactive products of the muon interactions with the scintillator have significant life times, that makes it impossible to use a muon tag. These isotopes are  $^{11}\text{Be}$  ( $\beta^-$ , 11.5 MeV, 13.8 s),  $^{10}\text{C}$  ( $\beta^+$ , 1.9 MeV +  $\gamma$ , 0.72 MeV, 19.3 s),  $^{11}\text{C}$  ( $\beta^+$ , 0.99 MeV, 20.38 min) and  $^7\text{Be}$  ( $\gamma$ , 0.478 MeV, 53.3 d). The considered neutrino window is too narrow to pick up a significant amount of events from these isotopes. Precise evaluations are now in progress for the Borexino detector [41], but this background will certainly be negligible in comparison to the other sources considered.

## 6 Neutrino signals

In the calculations we used SSM fluxes given by the standard solar model[42], neutrino energy spectra from [43]–[45] and survival probabilities for the LMA solar neutrino scenario from [46]. Signal shapes were convolved with the detectors response function using (3).

### 6.1 Sensitivity to the $pp$ -neutrinos.

The expected  $pp$ -neutrino count for the LMA solar neutrino oscillation scenario is listed in table 4. The sensitivity was estimated with the Monte Carlo (MC) method. First, the total signal was calculated taking into account the detector’s resolution. In the next step the normally distributed random signal was generated at each bin.

A fitting function consists of a function with 3 contributes describing the internal background (without  $^{14}\text{C}$ ), the spectrum of the  $^{14}\text{C}$  decay and the neutrino signal:

$$f(q) = N_{Bkg}Bkg(q) + N_{^{14}\text{C}} \cdot C(q) + N_{\nu}\phi_{\nu}(q) \quad (12)$$

The shape of the internal background  $Bkg(q)$  was fixed, but its normalization ( $N_{Bkg}$ ) was free. Another free parameter is the normalization of the  $^{14}\text{C}$  spectrum  $N_{^{14}\text{C}}$ .

The expected rates are listed in Table 4. The neutral current channel for the neutrinos of non- electron flavours are taken into account in the calculations. Other neutrino sources also have non- negligible contributions to the total signal in this energy window. The main source besides the  $pp$  are  $^7\text{Be}$  neutrinos with a flat spectrum (see Fig.2).

Using model (12) we find out that the total neutrino flux will be measured with 7.5% ( $1\sigma$ ) relative precision. Possible systematics errors due to the unknown shape of the background are not included in the estimation. We assume that the MC simulation can reproduce the form of the background and only the total normalization of this shape is unknown. The assumption is reasonable because of the quite narrow signal window, where the background is dominated by the slowly varying continuous spectrum of the soft part of the gamma spectra of radioactive impurities.

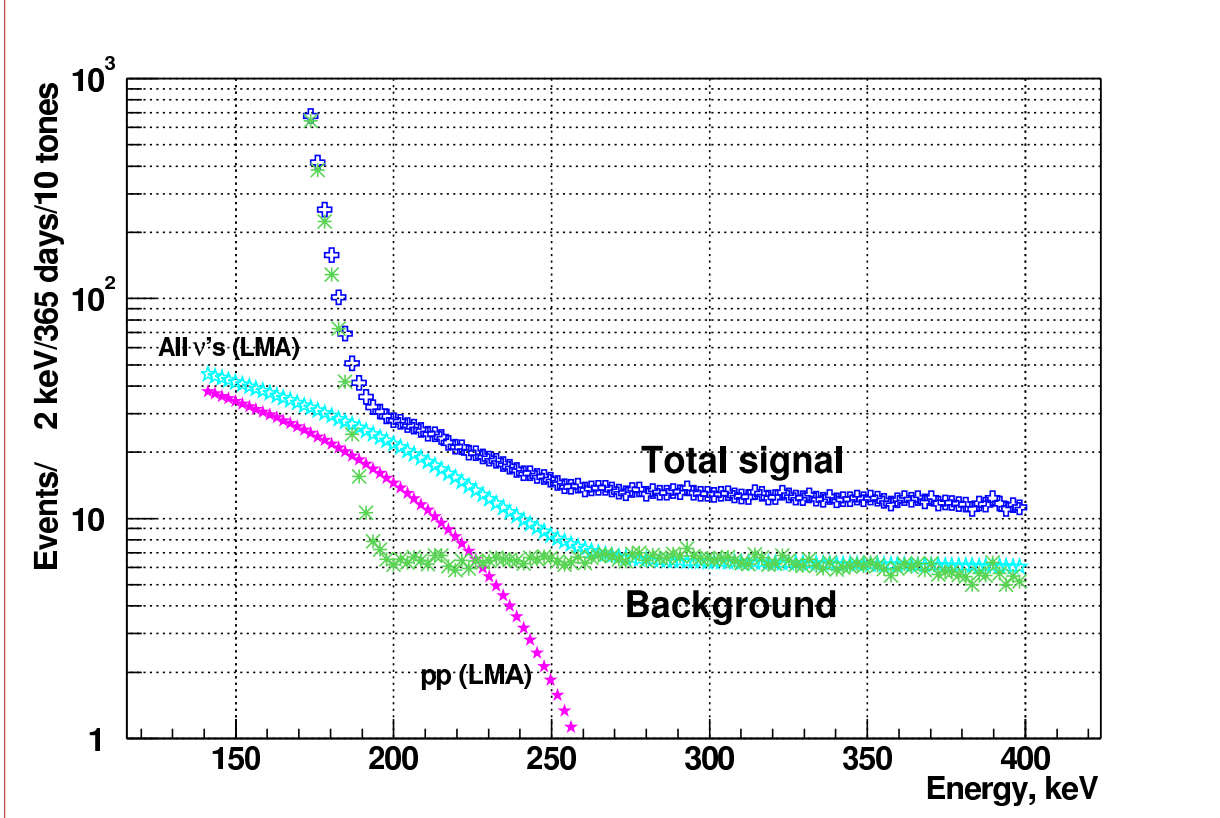


Figure 2: Signal and background shape for the SSM neutrino fluxes in the LMA MSW solution. The  $^{14}\text{C}$  content is  $2 \times 10^{-18} \text{g/g}$ . The concentrations of the main contributors to the background are listed in table. The detectors mass is 10 tons. The resolution is calculated with the assumption of 100% geometrical coverage using CTF-I light output for the liquid scintillator (i.e. 1800 p.e./MeV) and is assumed to be  $\frac{1}{\sqrt{N_{p.e.}}}$ . Shown signals correspond to 1 year of the data taking.

## 6.2 Sensitivity to $^7\text{Be}$ neutrinos

The detector will count 1070  $^7\text{Be}$  SSM LMA neutrinos per year in the 200–700- keV energy window with an internal background of 1130 events. For comparison, the Borexino detector will count 9390 events in the 250-750 keV energy window with a background of  $\sim 10500$  events. We are not presenting here the evaluation of the sensitivity of the detector to the  $^7\text{Be}$  neutrinos. It is clear that the lower mass (factor 10) with comparison to the Borexino detector will limit the sensitivity. A certain gain in the sensitivity can be achieved due to better energy resolution of the detector (factor 2.1). The sensitivity relative to Borexino for equal time of data taking and equal specific background can be estimated as  $\sqrt{\frac{M_{\text{Det}}}{M_{\text{Borex}}} \frac{\sigma_{\text{Borex}}}{\sigma_{\text{Det}}}} \simeq 0.45$  for the measurements on the edge of the recoil electrons of the  $^7\text{Be}$  neutrino (about 660 keV).

## 7 Improvement of the detector performances

The performance of the detector can be improved by using any of the following ideas:

1. **Use of the specially designed photomultipliers, providing better quantum efficiency.** The basic idea is the “recycling” of the incoming photons. Various optical arrangements have been used to improve light absorption by letting incoming light interact with the photocathode material more than once (see i.e. [47]). The idea has been revived in recent works [48],[49], where the authors reported significant increase of the quantum efficiency, up to a factor 2. There are also indications on the possibility of creating a photocathode with very high quantum efficiency using a material doped with nanoparticles [50].
2. **Use of the beta/gamma discrimination techniques.** The use of a different topology of the point-like beta events and the spatially distributed gamma- events can provide an opportunity to discriminate between beta and gamma induced signals with high efficiency. The method exploits the superior resolutions of the detector.
3. **Choice of the organic scintillator with lower content of  $^{14}C$ .** There are indications that the content of  $^{14}C$  can be much smaller than measured with the CTF-I detector, namely of the order of  $10^{-21}$  g/g [38]. In this case the  $^{14}C$  contribution in the background can be significantly reduced, and will lead to an improvement of the detector’s characteristics.

## 8 Conclusions

It is shown that a high energy resolution detector with the radiopurity levels necessary for the operation of Borexino, as well as solar neutrino project of KamLAND, will be sensitive to solar  $pp$ -neutrinos. The project can compete with other existing proposals (see Table 1).

This job would have been impossible without the support from the INFN sez. di Milano. We would like to thank Prof. G.Bellini and Dr. G.Ranucci for the continuous interest in our job.

We would like to thank all the colleagues from the Borexino collaboration for the pleasure to work together. Special thanks to R.Ford for the careful reading of the manuscript.

## References

- [1] K.Eguchi, et al, KamLAND collaboration, Phys.Rev.Lett. 90 (2003) 021802.
- [2] A.Bandyopadhyay, S.Choubey, R.Gandhi, S.Goswami, D.P.Roy, Phys.Lett. **B** 559 (2003) 121.



- [3] E.Calabresu, G.Fiorentini, and M.Lissia, astro-ph/9602045.
- [4] J.N.Bahcall, Proceedings Second International Workshop on Low Energy Solar Neutrinos, University of Tokyo, Japan, 2000.
- [5] S. Turck-Chieze, The Sun: a laboratory for determining neutrino properties, LowNu-2003 workshop, May 2003, Paris, <http://cdfinfo.in2p3.fr/LowNu2003/>.
- [6] R.S.Raghavan, LENS meeting at LNGS, Assergi, 28 July 1998; M.Fujiwara et al. arXiv:nucl-ex/0006006.
- [7] R.S.Raghavan, LENS. LowNu-2003 workshop, May 2003, Paris, <http://cdfinfo.in2p3.fr/LowNu2003/>.
- [8] H.V.Klapdor-Kleingrothaus, Nucl. Phys. B (Proc.Suppl.) **100**, 350, 2001. W. Hofmann/G. Heusser, Physics with naked Germanium in liquid Nitrogen, LowNu-2003 workshop, May 2003, Paris, <http://cdfinfo.in2p3.fr/LowNu2003/>.
- [9] R. Lanou, HERON, LowNu-2003 workshop, May 2003, Paris, <http://cdfinfo.in2p3.fr/LowNu2003/>.
- [10] M. Nakahata, XMASS, *ibid.*
- [11] A.Sarrat (on behalf of the HELLAZ collab.), Nucl. Phys. B (Proc.Suppl.) **95**, 177, 2001 .
- [12] H.Ejiri, Proc. Int. Workshop on Low Energy Solar Neutrinos, LowNu2, December 4 and 5, 2000, Tokyo, Japan, ed. by Y.Suzuki (World Scientific, Singapore, 2001), <http://www-sk.icrr.u-tokyo.ac.jp/neutlowe/2/transparency/index.html>
- [13] C.Broggini, *ibid.*
- [14] D.N. McKinsey, and J.M. Doyle, astro-ph/9907314.
- [15] J.N.Abdurashitov et al., Phys.Rev **C60**, 055801, 1999.
- [16] W.Hampel et al., Phys.Lett. B **447**, 127, 1999.
- [17] Smirnov O., Zaimidoroga O., Derbin A.  
Search for the solar  $pp$ -neutrinos with an upgrade of CTF detector.  
Phys.At.Nucl. Vol 66, No4 (2003) 712-723.
- [18] Arpesella C. et al., Borexino at Gran Sasso, Proposal for a real time detector for low energy solar neutrino.. Vol. 1. Edited by G.Bellini et al. (Dept. of Physics of the University of Milano, August 1991).
- [19] Alimonti G. et al., Astroparticle Physics **16**, 205, 2002.

- [20] Alimonti G. et al. , Nucl.Instrum.Methods **A 406**, 411, 1998.
- [21] Alimonti G. et al., Astroparticle Physics **8**, 141, 1998.
- [22] Borexino internal report, 2003.
- [23] Alimonti G. et al., Phys.Lett. **B 422**, 349, 1998.
- [24] O.Ju.Smirnov, Borexino Internal Note, 02/27/07.
- [25] G.Ranucci et al., Nucl.Instrum.Methods A **333**, 553, 1993.
- [26] Alimonti G. et al., Nucl.Instrum.Methods **A 440**, 360, 1998.
- [27] O.Ju.Smirnov, Instruments and Experimental Techniques, Vol 46, No 3 (2003) 327.
- [28] J.B.Birks, Proc.Phys.Soc. A64 (1951) 874.
- [29] J.M.Los Arcos, F.Ortiz, Comp.Phys.Comm. 103 (1997) 83.
- [30] Y. Kishimoto, KamLAND solar neutrinos, LowNu-2003 workshop, May 2003, Paris, <http://cdfinfo.in2p3.fr/LowNu2003/>.
- [31] Walter R. Nelson, Hideo Hirayama, David W. O. Rogers. The EGS4 code system. SLAC-265, 1985.
- [32] M.N.Peron. Private communication.
- [33] Silvia Bonetti. Private communication.
- [34] M.Morita, Beta Decay and Muon Capture (Benjamin, Reading, Mass., 1973) p. 33.
- [35] J.J.Simpson, and A.Hime, Phys.Rev. **39D**, 1825, 1989.
- [36] H.Behrens, and J.Janecke, Numerical Tables for Beta Decay and Electron Capture (Springer- Verlag, Berlin, 1969).
- [37] M.E.Rose, Phys.Rev. **49**, 727, 1936.
- [38] E. Resconi, Doct. Thesis, Universita' degli Studi di Genova, 2001; S.Schoenert, private communication.
- [39] Arpesella C. et al., Astroparticle Physics **18**, 1, 2002.
- [40] A. Ianni, G. Korga, G. Ranucci, et al., LNGS preprint INFN/TC-00/05.
- [41] T.Hagner, F.von Hentig, B.Heisinger et al., Astrop.Phys. **14**, 33, 2000.
- [42] J. N. Bahcall, H. Pinsonneault, and S. Basu, astro-ph/0010346.

- [43] J. N. Bahcall and R. K. Ulrich, Rev. Mod. Phys. **60**, 297, 1988.
- [44] J.N. Bahcall, E. Lisi, D.E. Alburger et al., Phys. Rev. **C 54**, 411,1996.
- [45] J.N. Bahcall, Phys. Rev. **C 56**, 3391, 1997.
- [46] J.N. Bahcall, Krastev, and A.Ju.Smirnov, Phys. Rev. **D 58**, 096016, 1998.
- [47] W.D.Gunter, Jr., G.R.Grant, and S.A.Shaw, Appl.Optics, **9**, No.2, 251, 1970.
- [48] S.Harmer, S.Hallensleben, and P.D.Townsend, Nucl.Instrum.Methods B **166-167**, 798, 2000.
- [49] S.Hallensleben, S.Harmer, P.D.Townsend, Optics Comm. **180**, 89, 2000.
- [50] I.E. Protsenko, V.N. Samoilov, O.A. Zaimidoroga. Russian Patent No 2002107248 with priority from 22/03/2002.